An observer design for the flux of line start permanent magnet synchronous motors

Hoang-Giang Vu

Electric Power University
Faculty of Electrical Engineering
235 Hoang Quoc Viet Street, Hanoi City, Vietnam

Abstract *– The flux generated by permanent magnets is essential to the performance of the line start permanent magnet synchronous motor (LSPMSM), especially during the start-up operation. The permanent magnet is degraded with operating time due to the demagnetization phenomenon, which is principally caused by the armature magnetic field interaction and operating temperature. In the motor model, the permanent magnet flux is important since it directly affects the electromagnetic torque. This paper introduces an observer design that is aimed at estimating the permanent magnet flux of the LSPMSM from the measurement of stator currents. First, derived from the mathematical equations of the motor in the dq0 reference frame, a set of equations in state variables of stator currents, magnetic fluxes and rotor angular frequency is considered. Equations of the fluxes are analyzed with the introduction of a new flux variable that allows designing open loops to estimate the fluxes from the stator currents. Moreover, a system of equations only in the state variables of stator currents and permanent magnet flux is formulated in order to design a flux observer, which is with a constant gain. Simulation results confirm the efficiency and robustness of the designed observer.*

1. INTRODUCTION

Facing the challenges of future energy demand and environmental issues during the process of exploiting and using fossil energy, many countries in the world have stepped up the transition to efficient and renewable energies. Besides promoting the development of power generation technologies using renewable energy, improving efficiency is an appropriate option that has received much attention in recent times.

In fact, about 50% of electricity consumed by electrical loads comes from electric motors [1]. In each country, electric motors consume about two-thirds of the electricity absorbed in the industry [2], [3]. Among various types of electric motors, induction motors are extensively used as industrial drives due to the basic features of simple structure, reliable operation and low cost. However, the huge drawback of this type of machine is its limited efficiency and low power factor.

As a more recent structural improvement in last decades, the line start permanent magnet synchronous motor (LSPMSM) is an alternative choice for the squirrel cage induction motor. The LSPMSM has a similar structure of squirrel cage induction motor, but permanent magnets are embedded in the rotor.

The LSPMSM has many advantages of high starting torque, high power factor grade and efficiency range.

In addition, the power drive with this type of motor is cost-effective since no inverter is required to be installed for the connection to the power source [3], [4]. Therefore, it is increasingly used in various applications where the machine is required to be directly powered by the main grid. For instance, it is applied in the system of pumps and fans in the mining industry [4]. The start-up moment of the LSPMSM is improved in comparison with that of the squirrel cage induction motor thanks to the installation of the permanent magnet into the rotor. Unexpectedly, the permanent magnet is suffered by the magnetic field generated by the armature winding and temperature [5], [6], [7]. The demagnetization may occur during the start-up of the machine, abnormal operation, and heavy load conditions that degrades the magnets [8].

The investigation of demagnetization phenomenon has been widely carried out to analyze the process of partial demagnetization of permanent magnets (PMs) and its influence on the performance of the LSPMSM. Most of the studies apply the finite element method (FEM) to solve the equation which is established from the model of coupled electromagnetic and thermal phenomena [4], [5], [7], [8], [9]. The authors in [5] proposed a model of coupled electromagnetic and thermal phenomena in a LSPMSM to analyze the effect of temperature on the magnetic, electrical and thermal properties of the materials. Furthermore, the modeling of

the process of partial demagnetization was presented. It was suggested to be used for the analysis of the effect of magnet demagnetization on the operation of the LSPMSM. In [7], a study of the demagnetization of the Nd-Fe-B magnet by an inclined field was shown. A FEM-based model was built to calculate the demagnetization of the LSPMSM under heavily loaded and overheated conditions. Finite element analysis (FEA) was also used in [8] for the investigation of demagnetization process, in which the decaying of the magnets' properties due to the impact of the demagnetizing magnetic motive force was taken into account. Furthermore, a FEM simulation model was utilized to calculate the remaining magnetization of the permanent magnet that has been exposed to high demagnetizing fields and/or temperature [9]. It was recommended that the average model intrinsic coercivity and the magnet remanence must be calibrated in order to achieve good agreement between simulation and experiment results.

For the permanent magnet synchronous motor (PMSM) in general, many detection methods for the demagnetization of PMs have been proposed, for instance, the techniques based on the spectral analysis of output data [10], [11]; the method using high-frequency signal injection [12]. Other methods are based on flux observer [13], [14], [15] that allow carrying out on-line detection technologies.

In the construction, the LSPMSM is structured with a hybrid rotor that includes a rotor cage like induction motors for the high starting torque and permanent magnets installed in the rotor like permanent magnet synchronous motors for the high efficiency [3]. As a result, in the model-based studies, the motor mathematical model seems to be more complex with the appearance of the permanent magnet flux and, as a consequence, the common difference between d-axis and q-axis parameters in dq0 reference frame. The permanent magnet flux is a modeling parameter that is often identified at the initial stage of an application and will be used for various purposes such as the analysis of system operation during the start-up and steady state, condition monitoring and fault diagnosis of the motor. Furthermore, as mentioned before, the flux can be degraded due to the demagnetization phenomenon. Therefore, the value of permanent magnet flux is very useful in both normal operation and condition monitoring of the LSPMSM. In this investigation, an observer-based approach is proposed to estimate the flux of the permanent magnet. Based on the original model of the motor in the dq0 reference frame, the system and observer models are appropriately formulated with the input of the stator voltages and rotor angular frequency, and the output of the stator currents. The designed observer provides with information on the permanent magnet flux that is useful for condition monitoring during the operation of LSPMSM.

The rest of the article is organized as follows. Section 2 presents the model of the LSPMSM in the dq0 refer-ence frame. Following this, the system and observer are formulated to observe the permanent magnet flux in section 3. Section 4 introduces the simulation results of the LSPMSM and its observer. Finally, the conclusion is given in Section 5.

2. MODEL OF LSPMSM

The model of the LSPMSM in the dq0 reference frame rotating with the rotor angular speed is given as [1], [16]:

$$v_{sd} = R_s i_{sd} + \frac{d\psi_{sd}}{dt} - \omega_r \psi_{sq} \tag{1}$$

$$v_{sq} = R_s i_{sq} + \frac{d\psi_{sq}}{dt} + \omega_r \psi_{sd} \tag{2}$$

$$v_{rd} = R_{rd} i_{rd} + \frac{d\psi_{rd}}{dt} = 0 \tag{3}$$

$$v_{rq} = R_{rq} i_{rq} + \frac{d\psi_{rq}}{dt} = 0 \tag{4}$$

$$\psi_{sd} = L_{sd} i_{sd} + L_{md} i_{rd} + \psi_m \tag{5}$$

$$\psi_{sq} = L_{sq} i_{sq} + L_{mq} i_{rq} \tag{6}$$

$$\psi_{rd} = L_{md} i_{sd} + L_{rd} i_{rd} + \psi_m \tag{7}$$

$$\psi_{rq} = L_{mq} i_{sq} + L_{rq} i_{rq} \tag{8}$$

where $L_{sd} = L_{ls} + L_{md}$, $L_{sq} = L_{ls} + L_{mq}$,

$L_{rd} = L_{lrd} + L_{md}$ and $L_{rq} = L_{lrq} + L_{mq}$.

In addition, the rotating equation of the LSPMSM is written by:

$$J \frac{d\omega}{dt} = T_e - T_m - T_f \tag{9}$$

where the electrical torque is computed by

$$T_e = \frac{3p}{2} \left(i_{sq} \psi_{sd} - i_{sd} \psi_{sq} \right). \tag{10}$$

In per unit system, equations from (1) to (9) become:

$$\frac{d\psi_{sd}}{dt} = \omega_b \left(v_{sd} - R_s i_{sd} + \omega_r \psi_{sq} \right) \tag{11}$$

$$\frac{d\psi_{sq}}{dt} = \omega_b \left(v_{sq} - R_s i_{sq} - \omega_r \psi_{sd} \right) \tag{12}$$

$$\frac{d\psi_{rd}}{dt} = -\omega_b R_{rd} i_{rd} \tag{13}$$

$$\frac{d\psi_{rq}}{dt} = -\omega_b R_{rq} i_{rq} \tag{14}$$

$$\psi_{sd} = L_{sd} i_{sd} + L_{md} i_{rd} + \psi_m \tag{15}$$

$$\psi_{sq} = L_{sq} i_{sq} + L_{mq} i_{rq} \tag{16}$$

$$\psi_{rd} = L_{md} i_{sd} + L_{rd} i_{rd} + \psi_m \tag{17}$$

$$\psi_{rq} = L_{mq} i_{sq} + L_{rq} i_{rq} \tag{18}$$

$$2H \frac{d\omega}{dt} = T_e - T_m - T_f \tag{19}$$

where all parameters are used in per unit system; motor inertia J becomes inertia constant H that is defined as $H = \dfrac{J\omega_{bm}{}^2}{2S_b}$ in which ω_{bm} is the base mechanical angular frequency; S_b is the base volt-ampere; and $T_e = i_{sq}\psi_{sd} - i_{sd}\psi_{sq}$.

$$\frac{d}{dt}i_{sd} = -a_{11}i_{sd} + a_{12}\omega i_{sq} + a_{13}\psi_{rdm} + a_{14}\omega\psi_{rq} + b_1 v_{sd} \tag{20}$$

$$\frac{d}{dt}i_{sq} = -a_{21}\omega i_{sd} - a_{22}i_{sq} - a_{23}\omega\psi_{rdm} + a_{24}\psi_{rq} - (a_{23} + a_{25})\omega\psi_m + b_2 v_{sq} \tag{21}$$

$$\frac{d\psi_{rdm}}{dt} = a_{31}i_{sd} - a_{33}\psi_{rdm} \tag{22}$$

$$\frac{d\psi_{rq}}{dt} = a_{42}i_{sq} - a_{44}\psi_{rq} \tag{23}$$

$$2H\frac{d\omega}{dt} = T_e - T_m - T_f \tag{24}$$

where new constants

$$a_{11}, a_{12}, a_{13}, a_{14}, a_{21}, a_{22}, a_{23}, a_{24}, a_{25}, a_{31}, a_{33}, a_{42}, a_{44}, b_1, b_2$$

are defined in Appendix B.

In equations from (20) to (22), a new definition is introduced that $\Psi_{rdm} = \Psi_{rd} - \Psi_m$. It will be shown in the next section that the fluxes of Ψ_{rdm} and Ψ_{rq} can be estimated via open loops.

To estimate the permanent magnet flux, the following equation is added:

$$\frac{d\psi_m}{dt} = 0 \tag{25}$$

Using the equation from (20) to (25), the model of system and observer will be formulated in the next section.

3. SYSTEM MODEL FORMULATION AND OBSERVER DESIGN

In this section, the system and observer models are formulated to design an observer for the estimation of the permanent magnet flux, Fig. 1.
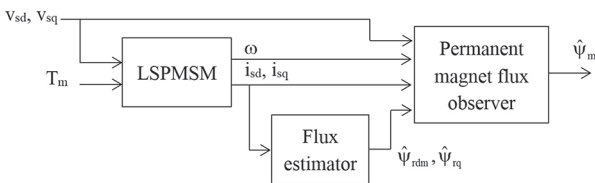
Fig. 1. Diagram of LSPMSM with the flux estimator and permanent magnet flux observer.

The LSPMSM is simulated with a detail diagram depicted in Fig.2. It is composed of the following main blocks:

- The top block is used to transform the grid voltage from a three-phase reference frame into the dq0 reference frame that rotates at the angular speed of the rotor;

- The three bottom blocks implement the model of the motor in the dq0 reference frame. First, the equations from (11) to (18) are used to calculate the components of stator currents and stator fluxes. They are then used for the computation of the electromagnetic torque (T_e). Finally, Equation (19) is utilized to calculate the speed and the angle of the rotor.
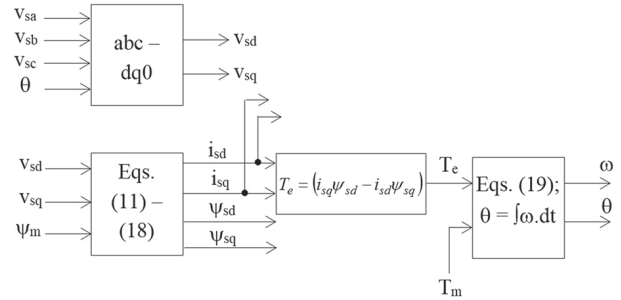
Fig. 2. Detailed diagram of LSPMSM simulation

Equivalently, the LSPMSM can be simulated by using equations from (20) to (24).

3.1. SYSTEM AND OBSERVER MODELS

The system model is established by using equations (20), (21), and (25):

$$\begin{cases} \dot{x} = A(u,x).x + B(u) = f(u,x) \\ y = x_1 = C.x \end{cases} \tag{26}$$

where x is the state, $x = [x_1\, x_2]^T$ with $x_1 = [i_{sd}\, i_{sq}]^T$ and $x_2 = \Psi_m$; $f(u,x) = [f_1(u,x)\, f_2(u,x)]^T$; y is the output; u is the input, $u = [v_{sd}\, v_{sq}\, \omega]^T$; and the matrices in the equation are given as

$$A(u,x) = \begin{bmatrix} -a_{11} & a_{12}\omega & 0 \\ -a_{21}\omega & -a_{22} & -(a_{23}+a_{25})\omega \\ 0 & 0 & 0 \end{bmatrix},$$

$$B(u) = \begin{bmatrix} a_{13}\hat{\psi}_{rdm} + a_{14}\omega\hat{\psi}_{rq} + b_1 v_{sd} \\ -a_{23}\omega\hat{\psi}_{rdm} + a_{24}\hat{\psi}_{rq} + b_2 v_{sq} \\ 0 \end{bmatrix}$$

and $C = \begin{bmatrix} 1 & 0 & 0 \\ 0 & 1 & 0 \end{bmatrix}$.

The fluxes of $\hat{\psi}_{rdm}$ and $\hat{\psi}_{rq}$ are estimated from the stator currents via open loops. In the next subsection, a simple proof will be described for the observation of these fluxes.

3.2. ESTIMATION OF FLUXES

Indeed, equations (22) and (23) are of the following form:

$$\frac{dz}{dt} = -a.z + b.y_z \qquad (27)$$

where z is the state, y_z is the output.

Note that if $y_z=0$ then equation (27) becomes:

$$\frac{dz}{dt} = -a.z \qquad (28)$$

It is clearly that if $a>0$ then z decay exponentially to 0 with any initial condition $z(0)$. With $y_z\neq0$, defining the estimation error of z as $\tilde{z}=z-\hat{z}$, the resulting estimation dynamic can be expressed by:

$$\frac{d\tilde{z}}{dt} = \frac{d(z-\hat{z})}{dt} = \left(-a.z + by_z\right) - \left(-a.\hat{z} + by_z\right)$$
$$= -a(z-\hat{z}) = -a\tilde{z}$$

or

$$\frac{d\tilde{z}}{dt} = -a.\tilde{z} \qquad (29)$$

Now, we can repeat for (29) from the analysis for (28). In conclusion, two separate open- loop flux estimators can be built:

$$\frac{d\hat{\psi}_{rdm}}{dt} = a_{31}i_{sd} - a_{33}\hat{\psi}_{rdm} \qquad (30)$$

$$\frac{d\hat{\psi}_{rq}}{dt} = a_{42}i_{sq} - a_{44}\hat{\psi}_{rq} \qquad (31)$$

3.3. OBSERVER FORM

From (26), differentiating $f_1 (u, x)$ with respect to x_2, we obtain $\dfrac{\partial f_1}{dx_2} = \begin{bmatrix} 0 \\ -(a_{23} + a_{25})\omega \end{bmatrix}$.

It is obviously seen that $\dfrac{\partial f_1}{dx_2}$ is located in a half plane when the rotor speed varies. Therefore, $A(u, x)$ is convex by (A_1 and A_2) where

$$A_1 = \begin{bmatrix} -a_{11} & a_{12}\omega_{min} & 0 \\ -a_{21}\omega_{min} - a_{22} & -(a_{23}+a_{25})\omega_{min} \\ 0 & 0 & 0 \end{bmatrix} \quad \text{and}$$

$$A_2 = \begin{bmatrix} -a_{11} & a_{12}\omega_{max} & 0 \\ -a_{21}\omega_{max} - a_{22} & -(a_{23}+a_{25})\omega_{max} \\ 0 & 0 & 0 \end{bmatrix}$$

in which the minimum and maximum values of ω can be respectively selected as $\omega_{min}=0$, $\omega_{max}=\omega_e/p$ where ω_e is the angular frequency of the main grid.

Therefore, a candidate of observer is of the following form [17], [18]:

$$\dot{\hat{x}} = A(u,\hat{x}).\hat{x} + B(u) + \Delta_\lambda K(Cx - y) \qquad (32)$$

where

$$\Delta_\lambda = \begin{bmatrix} \lambda & 0 & 0 \\ 0 & \lambda & 0 \\ 0 & 0 & \lambda^2 \end{bmatrix}$$

and $K=Q^{-1} C^T$ with Q is the solution of the following in-equality for A_1 and A_2:

$$QA + A^T Q - \rho C^T C \leq -\eta I \qquad (33)$$

In addition, the following inequalities are added to restrict gain matrix K:

$$I \leq Q \leq \zeta I$$
$$-\xi I \leq C'(QK) + (QK)C \leq \xi I \qquad (34)$$

where $\zeta>1$ and $\xi>0$.

Select $\eta=1$, $\rho=1$ then K is obtained by:

$$K = \begin{bmatrix} -4328 & -73 \\ -73 & -888 \\ 536 & 12 \end{bmatrix} \qquad (35)$$

Finally, by tuning, we obtain $\lambda=1$.

4. SIMULATION RESULTS AND DISCUSSION

In this section, the performance of the proposed observer is validated via simulation. The block diagram of the LSPMSM system with observer is given in Fig.1. The complete simulation block model developed in the Scilab/Xcos environment is given in Appendix C. The flux estimator uses only stator currents and provides estimated values of ψ_{rdm} and ψ_{rq} for the permanent magnet flux observer.

The simulation is developed in the following conditions:

• The LSPMSM is simulated using equations from (11) to (19);

• The motor parameters are given in Appendix A, which are adopted from [19];

• The initial condition to simulate LSPMSM is

$$\begin{bmatrix} \psi_{rd0} & \psi_{rq0} & i_{sd0} & i_{sq0} & \omega_{r0} & T_{m0} \end{bmatrix}$$
$$= \begin{bmatrix} 0.86 & 0 & -0.92 & 0.86 & 0 & 0.1 \end{bmatrix}$$

• The initial condition of estimator and observer respectively are:

$$\begin{bmatrix} \hat{\psi}_{rdm} & \hat{\psi}_{rq} \end{bmatrix}^T = \begin{bmatrix} -0.26 & 0.2 \end{bmatrix}^T$$
$$\text{and } \begin{bmatrix} \hat{i}_{sd} & \hat{i}_{sq} & \hat{\psi}_m \end{bmatrix}^T = \begin{bmatrix} 0 & 0 & 0.60 \end{bmatrix}^T ;$$

• The power source voltage has the amplitude that $V_m=1pu$, at the angular frequency that $\omega_e=1pu$.

The load fluctuation is generated by changing the load torque over a period of 5s, as shown in the top subfigure of Fig. 3. The motor starts working at load torque 0.1pu, then its load is increased to rated level $(T_m=1pu)$ at $t = 2.5s$. After a period of 1s operating at this level, the load torque is reduced to 0.5pu at $t = 3.5s$ and back to the rated level at $t = 4.5s$. In addition, the permanent magnet flux is assumed to be degraded and dropped by 30% at $t = 4s$, as can be seen in the bottom subfigure of Fig. 3.
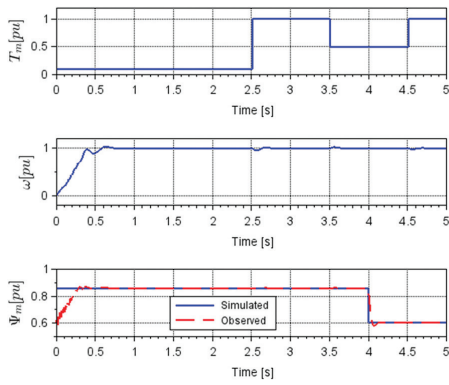
Fig. 3. Applied load torque (top); rotor speed (middle); and estimated permanent magnet flux (bottom)
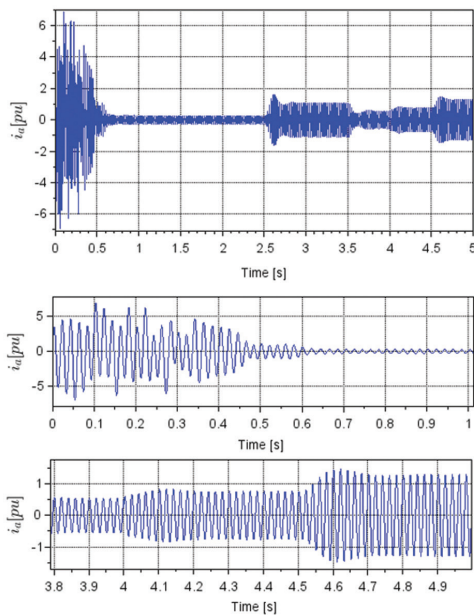
Fig. 4. The current of phase A (top); subfigure zoomed the start-up (middle); and subfigure zoomed the duration with sudden change of the permanent magnet flux (bottom)

The signal of phase stator current from the start-up to the synchronized operation with the main grid is shown in Fig. 4. It can be seen that the amplitude of the current varies due to the change of the load torque and the permanent magnet flux parameter.
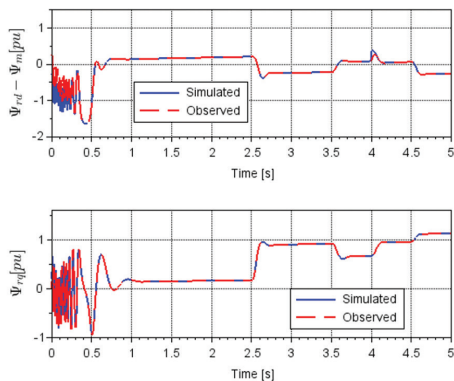
Fig. 5. Estimation results of ψ_{rdm} (upper) and ψ_{rq} (lower)

Fig. 5 shows the good estimation results for the fluxes ψ_{rdm} and ψ_{rq}, which are essential to the performance of the permanent magnet flux observer.
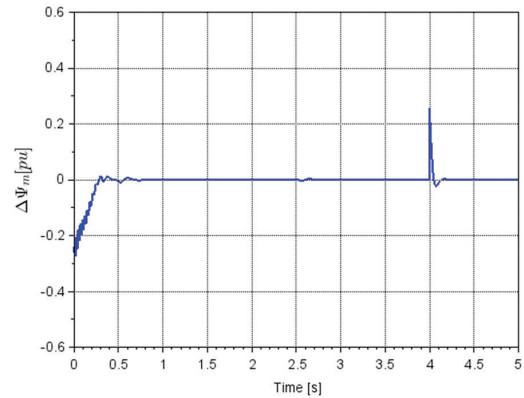
Fig. 6. Error between observed and simulated permanent magnet fluxes

Due to the load variation, the motor speed is slightly fluctuated around the events as can be viewed in the middle subfigure of Fig. 3. The speed is also influenced by the sudden change of the flux.

It can be seen in the bottom subfigure of Fig. 3 that the permanent magnet flux is well observed and the convergence is reached before the steady state of the system. The error between the estimated and simulated values is shown in Fig. 6. It robustly decays to zero after a sudden change of the permanent magnet flux. In addition, no error is recorded during the steady state, even with variations in load torque.

To evaluate the influence of parameters such as resistor uncertainty on the performance of the observer, the simulation is repeated under the condition that the resistor values used for the observer are set equal to 80% of the corresponding system parameters.

The estimated results and the error of permanent magnet flux are shown in the Figs 7 and 8, respectively.
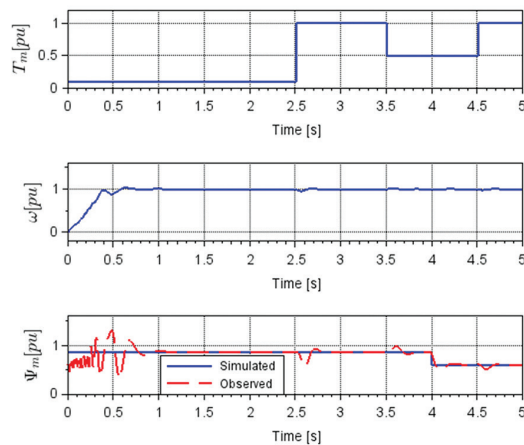
Fig. 7. Applied load torque (top); rotor speed (middle); and estimated permanent magnet flux (bottom) (resistance uncertainty)
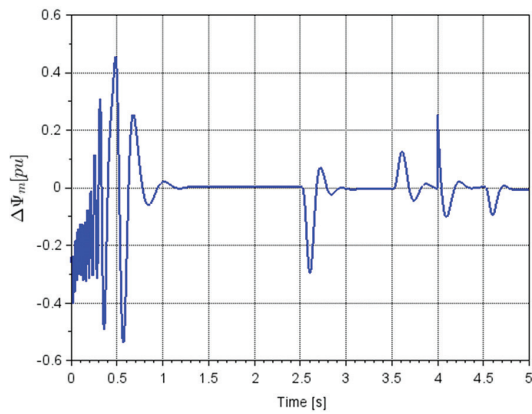
Fig. 8. Error between observed and simulated permanent magnet flux (resistance uncertainty)

It can be seen that the observer converges more slowly from the start with a larger estimation error. Furthermore, variations in load torque also cause the error; however, it is only significant around the time of the events. In steady state, the error is larger than that of the estimation with parameter certainty but insignificant.

The simulation results have illustrated the effective operation of the observer in the estimation of permanent magnet flux, even in the condition of parameter uncertainty. It must be reminded that the observer model in synchronous reference frame is characterized by robust computation with dc components of voltages, currents or fluxes.

In practice, a physical experiment platform can be implemented with a DSP driver board, a LSPMSM and power supply. Moreover, some sensors are needed for the information of stator currents, stator voltages, rotor position or rotor angular speed.

5. CONCLUSION

In this study, from the commonly mathematical model of LSPMSM, a model of the machine with the variables of stator currents, magnetic fluxes and rotor angular frequency was proposed. For the purpose of estimating the permanent magnet flux, a simple set of variables has allowed an open-loop estimation of the magnetic fluxes. In addition, an appropriate form of the observer with constant gain was obtained that provides robust performance in the estimation of the permanent magnet flux during different operation conditions of the motor. In order to obtain the flux information, three-phase voltage, three-phase current, rotor angular speed or rotor angular position information are needed. An on-line detection method can be introduced by applying the proposed flux observer that allows evaluating the demagnetization of the magnets for the condition monitoring of the LSPMSM.

6. ACKNOWLEDGEMENTS

7. LIST OF SYMBOLS

f_n	Rated frequency,
H	Inertia constant (pu)
i_{rd} and i_{rq}	Rotor currents in d-axis and q-axis referred to stator side,
i_{sd} and i_{sq}	Stator currents in d-axis and q-axis,
J	Motor inertial,
L_{lrd} and L_{lrq}	Rotor leakage inductances in the d- and q-axis referred to the stator side,
L_{ls}	Leakage stator inductance,
L_{md} and L_{mq}	Mutual inductances in the d- and q-axis,
L_{rd} and L_{rq}	Rotor total inductances in the d- and q-axis referred to the stator side,
L_{sd} and L_{sq}	Stator total inductances in the d- and q-axis,
ω	Rotor mechanical angular frequency,
ω_r	Rotor electrical angular frequency, $\omega_r = p.\ \omega$,
p	Number of pole pairs,
P_n	Rated power,
ψ_m	Flux of the permanent magnet refer to stator side,
ψ_{rd} and ψ_{rq}	Rotor leakages fluxes in d-axis and q-axis referred to stator side,
ψ_{sd} and ψ_{sq}	Stator leakage fluxes in d-axis and q-axis,
R_s	Stator resistance per phase,
R_{rd} and R_{rq}	Rotor resistances per phase in d-axis and q-axis referred to stator side,
T_f	Frictional torque,
T_m	Load torque,
V_n	Rated voltage,
v_{rd} and v_{rq}	Rotor voltages in d-axis and q-axis referred to stator side,
v_{sd} and v_{sq}	Stator voltages d-axis and q-axis.

8. APPENDIX

A. Parameters of LSPMSM

Nominal Parameter	Value
f_n	50 Hz
P_n	750 W
V_n	230 V
Model parameter	**Value**
H	0.3 pu
L_{lrd}	0.132 pu
L_{lrq}	0.132 pu
L_{ls}	0.065 pu
L_{sd}	0.543 pu
L_{sq}	1.086 pu
ψ_m	0.86 pu
R_{rd}	0.054 pu
R_{rq}	0.108 pu
R_{rs}	0.017 pu

B. Definition of constants in equations from (20) to (23)

$$\sigma_d = L_{sd} - \frac{L_{md}^2}{L_{rd}}; \quad a_{11} = \omega_b \frac{R_s + R_{rd}\frac{L_{md}^2}{L_{rd}^2}}{\sigma_d};$$

$$a_{12} = \omega_b \frac{p\left(L_{sq} - \frac{L_{mq}^2}{L_{rq}}\right)}{\sigma_d}; \quad a_{13} = \omega_b \frac{R_{rd}\frac{L_{md}}{L_{rd}^2}}{\sigma_d};$$

$$a_{14} = \omega_b \frac{p\frac{L_{mq}}{L_{rq}}}{\sigma_d}; b_1 = \omega_b \frac{1}{\sigma_d}; \sigma_q = L_{sq} - \frac{L_{mq}^2}{L_{rq}};$$

$$a_{21} = \omega_b \frac{p\left(L_{sd} - \frac{L_{md}^2}{L_{rd}}\right)}{\sigma_q}; \quad a_{22} = \omega_b \frac{R_s + R_{rq}\frac{L_{mq}^2}{L_{rq}^2}}{\sigma_q};$$

$$a_{23} = \omega_b \frac{p\frac{L_{md}}{L_{rd}}}{\sigma_q}; \quad a_{24} = \omega_b \frac{R_{rq}\frac{L_{mq}}{L_{rq}^2}}{\sigma_q}; \quad b_2 = \omega_b \frac{1}{\sigma_q}$$

$$a_{25} = \omega_b \frac{p\left(1 - \frac{L_{md}}{L_{rd}}\right)}{\sigma_q}; \quad a_{31} = \omega_b \frac{R_{rd}L_{md}}{L_{rd}}; \quad a_{33} = \omega_b \frac{R_{rd}}{L_{rd}}; ;|$$

$$a_{42} = \omega_b \frac{R_{rq}L_{mq}}{L_{rq}}; \quad a_{44} = \omega_b \frac{R_{rq}}{L_{rq}};$$

C. Simulation block model of LSPMSM and observer
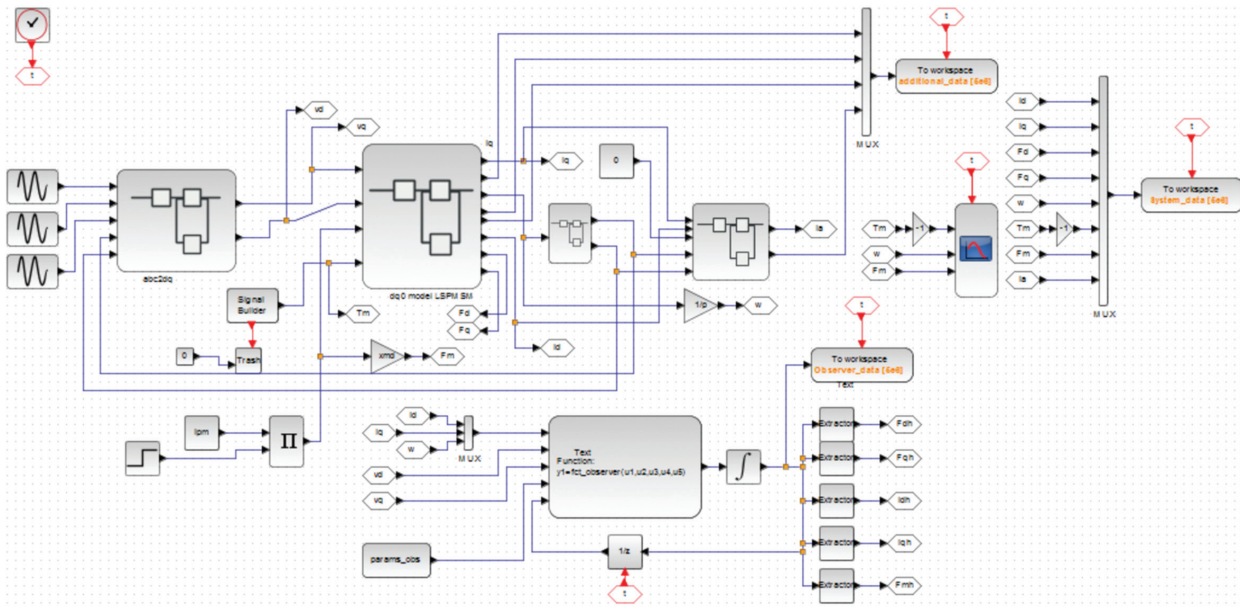
9. REFERENCES

[1] A. H. Sfahani, S. Vaez-Zadeh, "Line start permanent magnet synchronous motors: Challenges and opportunities", Energy, Vol. 24, No. 11, 2009, pp. 1755-1763.

[2] R. Saidur, "A review on electrical motors energy use and energy savings", Renewable and Sustainable Energy Reviews, Vol. 14, No. 3, 2010, pp. 877-898.

[3] M. R. Mehrjou, N. Mariun, N. Misron, M. A. M. Radzi, "Analysis of statistical features based on start-up

current envelope for broken rotor bar fault detection in line start permanent magnet synchronous motor", Electrical Engineering, Vol. 99, No. 1, 2017, pp. 187-201.

[4] M. Baranski, W. Szelag, W. Lyskawinski, "Analysis of the Partial Demagnetization Process of Magnets in a Line Start Permanent Magnet Synchronous Motor", Energies, Vol. 13, No. 21, 2020, p. 5562.

[5] M. Baranski, W. Szelag, W. Lyskawinski, "Experimental and simulation studies of partial demagnetization process of permanent magnets in electric motors", IEEE Transactions on Energy Conversion, Vol. 36, No. 4, 2021, pp. 3137-3145.

[6] S. Ruoho, J. Kolehmainen, J. Ikaheimo, A. Arkkio, "Interdependence of demagnetization, loading, and temperature rise in a permanent-magnet synchronous motor", IEEE Transactions on Magnetics, Vol. 46, No. 3, 2009, pp. 949-953.

[7] S. Ruoho, A. Arkkio, "Partial demagnetization of permanent magnets in electrical machines caused by an inclined field", IEEE Transactions on Magnetics, Vol. 44, No. 7, 2008, pp. 1773-1778.

[8] J. X. Shen, P. Li, M. J. Jin, G. Yang, "Investigation and countermeasures for demagnetization in line start permanent magnet synchronous motors", IEEE Transactions on Magnetics, Vol. 49, No. 7, 2013, pp. 4068-4071.

[9] S. Sjökvist, S. Eriksson, "Experimental verification of a simulation model for partial demagnetization of permanent magnets", IEEE Transactions on Magnetics, Vol. 50, No. 12, 2014, pp. 1-5.

[10] M. Krichen, E. Elbouchikhi, B. Naourez, M. Chaieb, R. Neji, "Motor current signature analysis-based permanent magnet synchronous motor demagnetization characterization and detection", Machines, Vol. 8, No. 35, 2020.

[11] C. Candelo-Zuluaga, J. Riba, D. Thangamuthu, A. Garcia, "Detection of partial demagnetization faults in five-phase permanent magnet assisted synchronous reluctance machines", Energies, Vol. 13, No. 13, 2020, p. 3496.

[12] J. Hong, "Detection and classification of rotor demagnetization and eccentricity faults for PM synchronous motors", IEEE Transactions on Industry Applications, Vol. 48, 2012, p. 923–932.

[13] Y. Min, W. Huang, J. Yang, Y. Zhao, "On-line estimation of permanent-magnet flux and temperature rise in stator winding for PMSM", in Proceedings of the 22nd International Conference on Electrical Machines and Systems, Harbin, China, 11–14 August 2019.

[14] X. Xiao, C. Chen, "Reduction of torque ripple due to demagnetization in PMSM using current compensation", IEEE Transactions on Applied Superconductivity, Vol. 20, 2010, pp. 1068-1071.

[15] L. Cao, Z. Wu, "On-Line Detection of Demagnetization for Permanent Magnet Synchronous Motor via Flux Observer", Machines, Vol. 10, No. 5, 2022, p. 354.

[16] L. Maraaba, Z. Al-Hamouz, A. Milhem, S. Twaha, "Comprehensive Parameters Identification and Dynamic Model Validation of Interior-Mount Line-Start Permanent Magnet Synchronous Motors", Machines, Vol. 7, No. 4, 2019.

[17] H.-G. Vu, H. Yahoui, H. Hammouri, "Nonlinear Observer Design for Load Torque Estimation of Induction Motors", Advances in Electrical and Electronic Engineering, Vol. 18, No. 3, 2020.

[18] H. Hammouri, M. Farza, "Nonlinear observers for locally uniformly observable systems", ESAIM. COCV, Vol. 9, pp. 353-370, 2003, pp. 153-159.

[19] M. A. Rahman, T. A. Little, "Dynamic performance analysis of permanent magnet synchronous motors magnet synchronous motors", IEEE Transactions on Power Apparatus and Systems, Vol. 6, 1984, pp. 1277-1282.